Oceanologia 64 (2022) 445—456

Available online at www.sciencedirect.com

ScienceDirect

journal homepage: www.journals.elsevier.com/oceanologia

ORIGINAL RESEARCH ARTICLE

Tropical cyclone intensity modulated by the oceanic eddies in the Bay of Bengal

Navaneeth Kodunthirapully Narayanaswami[a,b,*], **Venkatesan Ramasamy**[a]

[a] *Ocean Observation Systems, National Institute of Ocean Technology (NIOT), Chennai, India*
[b] *Anna University, Guindy Campus, Chennai, India*

Received 22 June 2021; accepted 20 February 2022
Available online 7 March 2022

KEYWORDS
Phailin;
Fani;
Eddy feedback factor;
Cold-core eddy;
Warm-core eddy

Abstract The Bay of Bengal, an affluent region for mesoscale oceanic eddies, is also home to devastating tropical cyclones. The intensity modulation of two cyclones, Phailin (2013) and Fani (2019), in the Bay of Bengal by the oceanic eddies is studied. The intensities of both the cyclones rapidly changed after transiting over mesoscale eddies. The surface and subsurface oceanic conditions before and during the passage of the two cyclones were analysed. During Phailin (Fani), the cyclonic (anticyclonic) eddy resulted in significant (weak) sea surface temperature cooling due to the shallow (deep) D26 isotherm. Wind shear estimates revealed that it had no (minor) effect on the weakening (intensification) of Phailin (Fani). The analysis of enthalpy fluxes during the two cyclones has shown that during Phailin (Fani), the latent heat flux supply was reduced (enhanced) by 20 W m^{-2} (30 W m^{-2}) over the regions of the cyclonic (anticyclonic) eddy due to significant (weak) sea surface temperature cooling. The case study of cyclone interaction with mesoscale oceanic eddies has shown that a thorough understanding of mesoscale eddies is vital for improving the accuracy of the cyclone intensity forecasts.

1. Introduction

Tropical cyclones (TCs) affect millions of people annually across the globe. TCs cause significant damage to life and property because of strong winds, heavy precipitation, and storm surge. Global warming has resulted in an increase in the frequency and intensity of TCs (Emanuel, 2013). The accurate forecast of TC, both in terms of its intensity and track, is highly critical for mitigating socio-economic impacts. Rappaport et al. (2012) reported that even though forecasting skills have improved in accurately predicting

* Corresponding author at: Ocean Observation Systems, National Institute of Ocean Technology (NIOT), Chennai 600025, India.
E-mail address: nkn968@gmail.com (N. Kodunthirapully Narayanaswami).
Peer review under the responsibility of the Institute of Oceanology of the Polish Academy of Sciences.

Production and hosting by Elsevier

https://doi.org/10.1016/j.oceano.2022.02.005

TC's track over the past few decades, intensity prediction remains challenging. The intensity change of a TC is governed by a multitude of atmospheric and oceanic processes. Emanuel et al. (2004) reported that air-sea interactions are highly crucial in controlling the intensity of TC. Sea Surface Temperature (SST) cooling induced by the strong TC winds can curtail the supply of enthalpy fluxes and impede the further intensification of TC (Cione and Uhlhorn, 2003; Halliwell et al., 2015). However, studies (Lloyd and Vecchi, 2011; Mei and Pasquero, 2013) have documented that the SST response to a TC is not entirely dependent on TC characteristics but also depends on the oceanic environment.

The oceanic environment is non-homogeneous. The mesoscale oceanic eddies have a significant role in determining the ocean's vertical temperature and salinity structure. Cyclonic (anticyclonic) eddies promote (restrain) SST cooling (Jaimes and Shay, 2009; Lin et al., 2005). Hence, the cyclonic (anticyclonic) eddies are referred to as cold (warm) core eddies. The intensification (weakening) of TCs over anticyclonic (cyclonic) eddies has been documented in several studies (Demaria and Kaplan, 1994; Liang et al., 2018, 2016; Lin et al., 2005; McTaggart-Cowan et al., 2006; Shay et al., 2000). Lin et al. (2005) have reported on Typhoon Maemi's rapid intensification over a giant warm-core eddy. Similarly, Ma et al. (2020) documented the mechanisms responsible for the unusual rapid weakening of typhoon Francisco over a cold-core eddy using observations and modelling studies.

The Bay of Bengal (BoB), a semi-closed marginal sea located in the tropical north-eastern Indian Ocean, is rich in mesoscale eddies (Babu et al., 2003; Chen et al., 2012; Cheng et al., 2013; Hacker et al., 1998; Kurien et al., 2010; Prasanna Kumar et al., 2004, 2007). Chen et al. (2012) reported that the majority of eddies in the BoB are generated in the eastern and western boundaries. Cheng et al. (2018) utilised the synergy of observations and models to understand eddy generation in the central BoB. They reported that equatorial zonal winds mainly drive eddies generated near the eastern BoB boundary. However, the eddy formation in the western BoB is attributed to the instability of flow in the East India Coastal Current (EICC) (Kurien et al., 2010). Vinayachandran (2013) also reported the formation of cold-core and warm-core eddies, especially during April, May, October, and November. The BoB is also home to the deadliest cyclones in history. High SSTs (~28–31°C) and weak vertical wind shear during pre-monsoon (Neetu et al., 2019) and high relative humidity during post-monsoon (Li et al., 2013) provide a conducive environment for TC formation in the BoB. Due to the funnel-shaped coastline, high storm surges generated during TC result in a high death toll. For example, the Orissa Super Cyclone resulted in the deaths of approximately 10,000 people. Hence, any errors in the forecasts of TC can have widespread socio-economic impacts.

The interaction between pre-existing mesoscale eddies and TCs in the BoB is a thrust area of research. Lin et al. (2009) investigated the intensification of Nargis over the warm ocean and reported that the pre-existing deep, warm subsurface layer decreased SST cooling induced by the TC. As a result, the enthalpy fluxes have been shown to increase by 300%. Sadhuram et al. (2012) documented the intensification of TC Aila by 43% over a warm-core eddy. Recently, Liu et al. (2021) documented the influence of pre-existing cold and warm-core eddies on the intensity of tropical storm Roanu in the BoB. Here, we investigate the intensity modulation of two intense TCs, Phailin (2013) and Fani (2019), in the BoB. Both the TCs interacted with pre-existing mesoscale eddies in the BoB before landfall. Phailin, a category-5 TC, encountered a cyclonic eddy and weakened to a category-3 TC before landfall. Contrastingly, Fani intensified to a category-4 TC from category-3 when it passed over an anticyclonic eddy. The role of pre-existing mesoscale eddies in the intensity modulation of these two intense TCs, Phailin (2013) and Fani (2019), in the BoB, was analysed and presented.

2. Data and methodology

The gridded daily global estimates of sea level anomaly (SLA) based on Ssalto/Duacs altimeter products produced and distributed by Copernicus Marine and Environment Monitoring Service (CMEMS) (http://www.marine.copernicus.eu) are used for the detection of mesoscale features. The six-hour interval tracks of Phailin (2013) and Fani (2019) were obtained from Joint Typhoon Warning Centre (https://www.metoc.navy.mil/jtwc/jtwc.html?north-indian-ocean). The high-resolution (1 km) daily-mean foundation SST (SSTfnd) from the Group for High-Resolution Sea Surface Temperature (GHRSST) Level 4 gridded products (Donlon et al., 2007) is utilised. Subsurface temperature data products at 1/12° resolution from CMEMS(http://marine.copernicus.eu/getting-started/) are used for the estimation of the depth of 26°C isotherms (D26) and Tropical Cyclone Heat Potential (TCHP). CMEMS products utilise the synergy of advanced modelling and data assimilation techniques.

The TCHP is calculated using the formula

$$\mathrm{TCHP} = \rho C p \int_0^{D26} (Tz - 26) dz \quad (1)$$

Hourly datasets of relative humidity at 700 hPa (MTRH), zonal and meridional winds at 200 and 850 hPa, Latent Heat Flux (LHF) and Sensible Heat Flux (SHF) from ERA5 reanalysis products (Hersbach and Dee, 2016) were also utilised. The in-situ observations of Sea Level Pressure (SLP), wind speed, and temperature profiles during TCs Phailin and Fani from moored buoys deployed by the National Institute of Ocean Technology (Venkatesan et al., 2013) are used for understanding the temporal evolution. Vertical Wind Shear (VWS) is calculated as the vector difference between the 200- and 850-hPa winds.

3. Results and discussion

3.1. Synopsis of cyclone Phailin (2013) and Fani (2019)

The track of the two intense TCs, Phailin (category-5) and Fani (category-4), developed over the BoB overlaid on TRMM rainfall along with the location of moored buoys deployed by the NIOT is shown in Figure 1a–b, respectively. North-central BoB received cumulative precipitation of ~20 cm

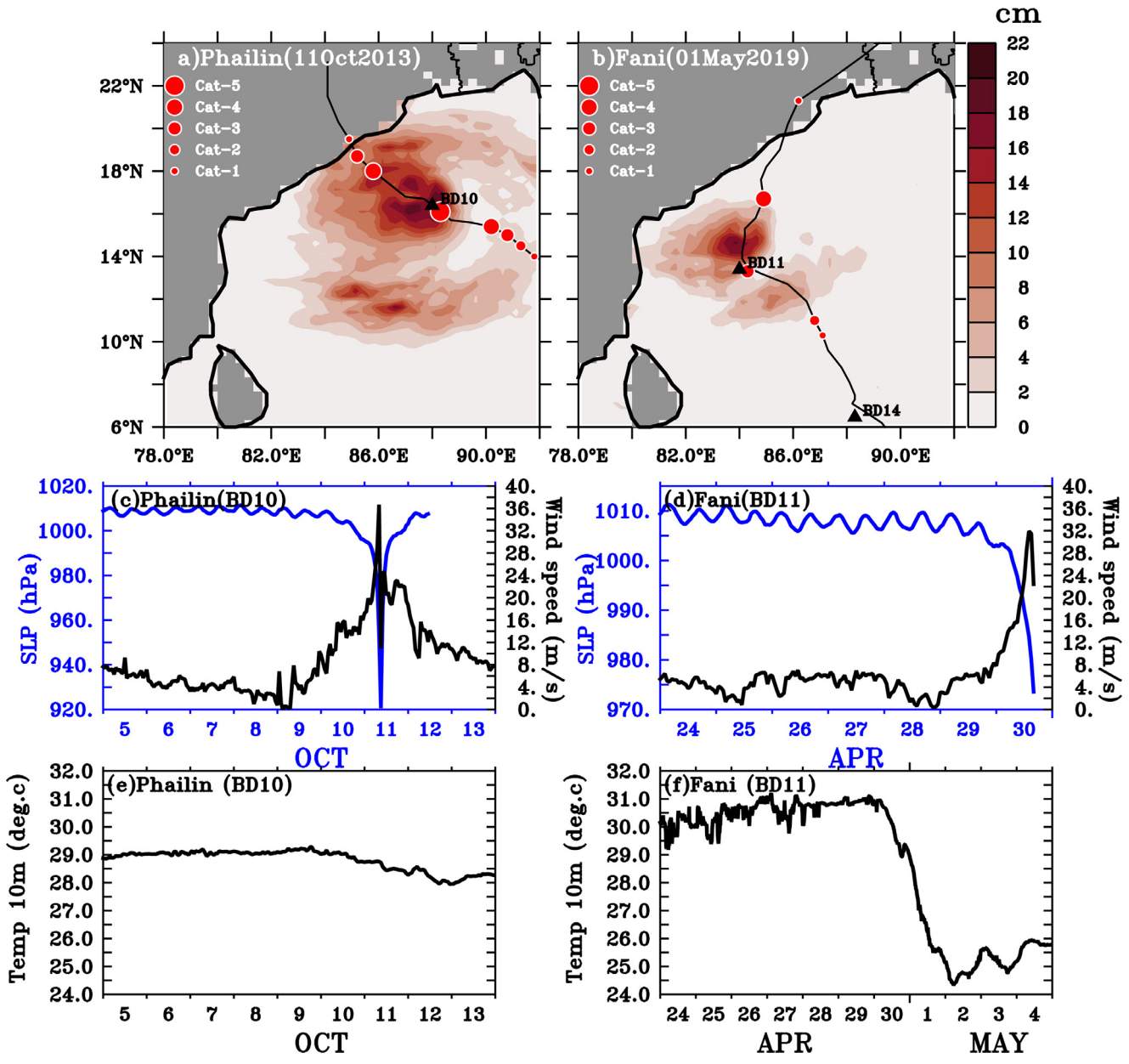

Figure 1 TRMM cumulative precipitation (cm) in the Bay of Bengal on (a) 11 October 2013 (Phailin), (b) 01 May 2019 (Fani). SLP and Wind speed at 10 m height (c) for Phailin, (d) for Fani. Subsurface temperature at 10 m from (e) BD10 for Phailin (f) BD11 for Fani. The black triangular shaped markers in panels a and b represent the mooring deployed by NIOT. The red circle-shaped markers in panels a and b indicate the intensity of the cyclone on Saffir-Simpson scale.

during Phailin. Phailin was the strongest post-monsoon cyclone (09—13 October 2013), making landfall at the Odisha coast after the Orissa Super Cyclone in 1999. Phailin developed as a tropical storm over the northern Andaman Sea on October 9, 2013 and intensified into a category-1 on October 10, 2013. Moving north-westwards, it further intensified into a category-3 TC and finally reached maximum intensity with a central pressure of 940 hPa and wind speed of 115 knots (category-5) on October 11, 2013 at 16.0°N, 88.5°E. It crossed Odisha near Gopalpur on 12 October 2013 as a category-3 cyclone. Fani (27 April—03 May 2019) was one of the strongest pre-monsoon TCs in the BoB after 1994, developed near the equator in the north Indian Ocean. Fani covered 3030 km in the open ocean from the south BoB to the north Odisha coast and maintained a wind speed of ≥100 knots for 36 hours (Singh et al., 2021). Heavy rainfall (~20 cm) occurred in the western BoB near the BD11 mooring (Figure 1b). It made landfall on the Odisha coast near Puri as a category-4 cyclone with ~105 knots.

3.2. In situ observations from moored buoys in the vicinity of cyclone track

The significant observations of meteorological parameters and SST from the moored buoys during Phailin and

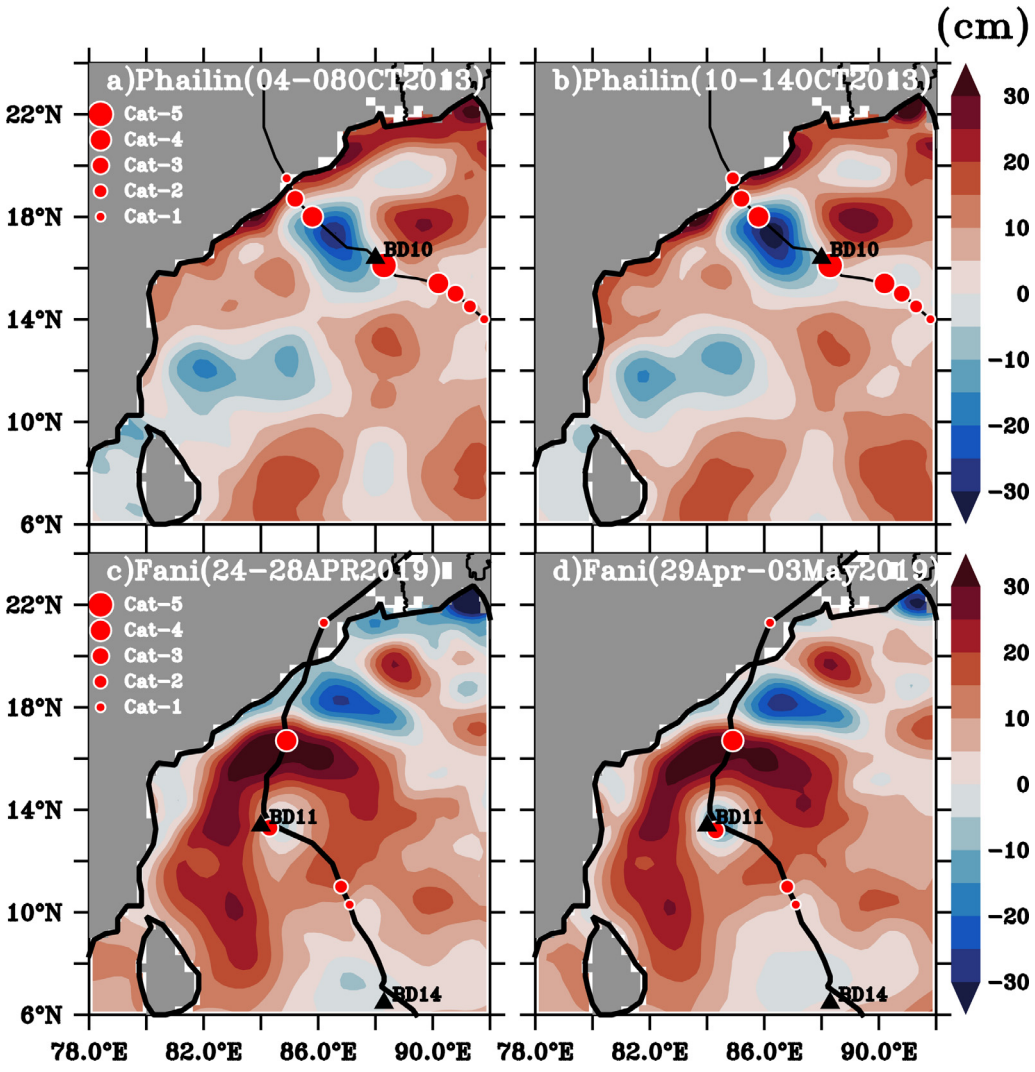

Figure 2 Five-day average AVISO SLA data (a) during 04—08 October 2013 before the passage of Phailin, (b) during 10—14 October 2013 during the passage of Phailin, (c) during 24—28 April 2019 before the passage of Fani, and (d) during 29 April—03 May 2019 during the passage of Fani. The black triangular shaped markers represent the moorings deployed by NIOT. The red circle-shaped markers indicate the intensity of the cyclone on the Saffir-Simpson scale.

Fani in the vicinity of the TC tracks were shown in Figure 1c—f. The average SLP was ~1010 hPa with wind speed in the range of 5—10 m s^{-1} before the passage of Phailin (Figure 1c). The SLP in the moored buoy BD10 (88°E/16.5°N) dropped to 920 hPa, and wind speeds increased to 37 m s^{-1} on 11 October 2013. The observations from remote sensing platforms also estimated the SLP to be around 910 hPa during Phailin. Note that Phailin was a category-5 cyclone near BD10. Two of the NIOT buoys, namely BD14 (88°E/7°N) and BD11 (84°E/13.5°N) along the track, recorded the significant anomalies of Fani (Figure 1d). BD14, located 35 km from the track, observed a maximum wind speed of 21 m s^{-1}, and SLP dropped to 997 hPa on 27 April 2019 during the genesis stage of Fani. The SLP dropped to 973.5 hPa, and the wind speed increased up to 32 m s^{-1} in BD11 (located 12 km from the track) on 30 April 2019, when Fani reached the intensity of category-3.

The temperature at 10 m from BD10 and BD11 during Phailin and Fani is shown in Figures 1e and f, respectively. The temperature measured at 10 m by the NIOT buoys can be considered Foundation SST (SSTfnd) since it is free from diurnal variability (GHRSST-PP). The SSTfnd from BD10 before Phailin was ~29—29.5°C (Figure 1e), whereas a high SSTfnd of ~30—31°C was observed at BD11 prior to the formation of Fani (Figure 1f). Intense cooling of ~6°C was observed at BD11 after the passage of Fani. However, SST cooling of ~1°C was observed at BD10 after Phailin's passage. Significant wave height of 6.8 m, 3.8 m and 5 m was recorded by the moored buoys BD11, BD14 and BD08, respectively, during Fani (Figures not shown). The synoptic conditions during the two TCs were analysed using remote sensing observations in the following section.

3.3. Surface oceanic conditions during Phailin and Fani

3.3.1. Pre-existing oceanic eddies

The presence of mesoscale oceanic eddies characterises the surface oceanic conditions before and during the passage of

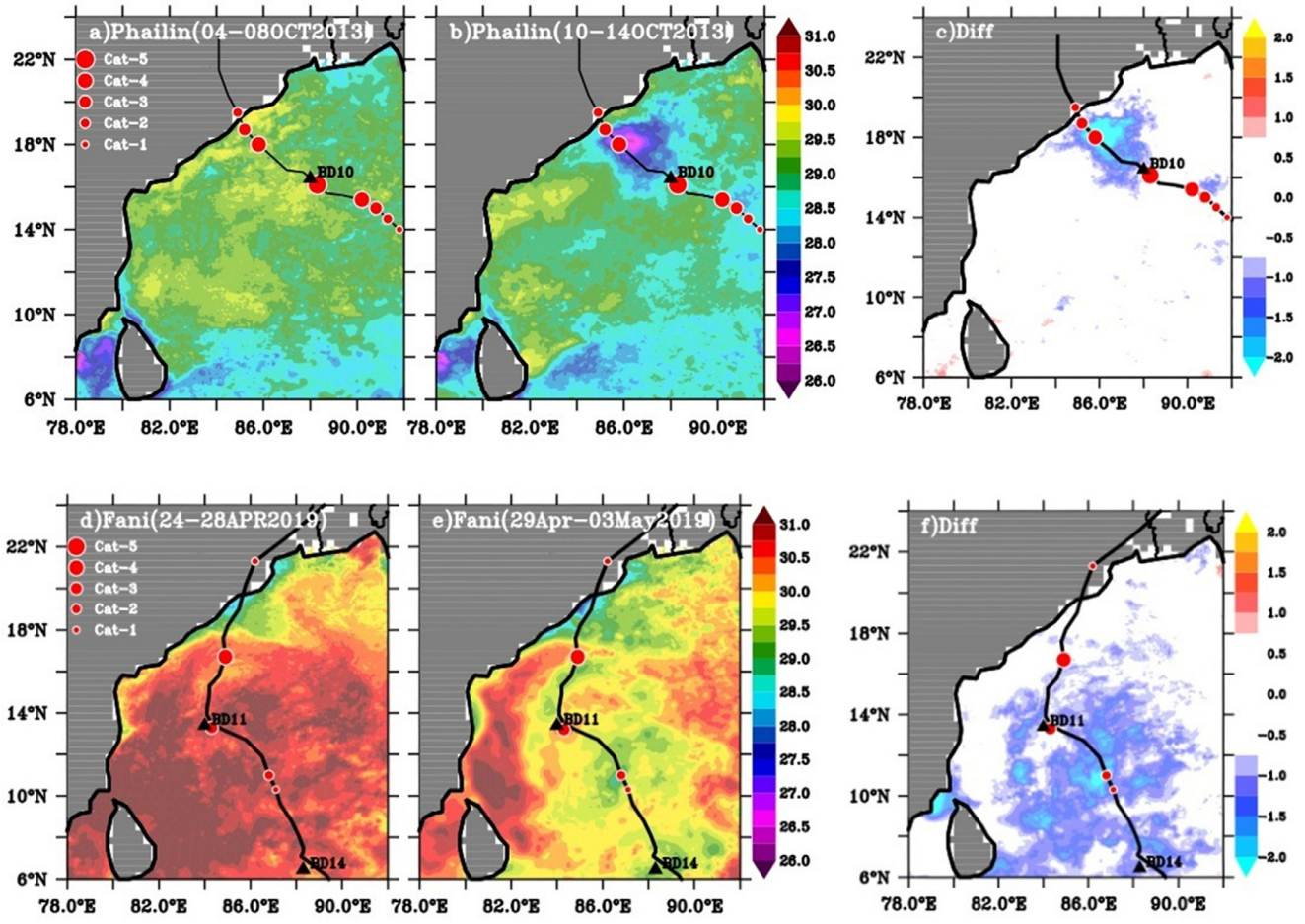

Figure 3 Five-day mean SST from GHRSST in the Bay of Bengal during (a) pre-Phailin days (04—08 October 2013), (b) Phailin days (10—14 October 2013), (d) pre-Fani days (24—28 April 2019), and (e) Fani days (29 April—03 May 2019). (c) SST changes caused by cyclone Phailin are calculated by subtracting SST data in (a) from (b). (d) The same as 3(c), but the SST changes after Fani's passage. The black triangular-shaped markers represent the moorings deployed by NIOT. The red circle-shaped markers indicate the intensity of the cyclone on the Saffir-Simpson scale.

Phailin and Fani. Mesoscale eddies are an integral part of ocean circulation in the BoB. Intense eddy activity is observed throughout the year in the BoB (Chen et al., 2012; Cheng et al., 2018). Eddies that are generated in the eastern BoB due to the interactions of wind, nonlinear processes, and coastline geometry get embedded in the Rossby waves and propagate westwards. The eddy also gets generated in the western BoB due to flow instabilities in the EICC (Kurien et al., 2010). Hence, the circulation in the western BoB is primarily dominated by eddy—mean flow interactions (Chen et al., 2012). TCs are most active in the BoB during the post-monsoon (October—December) and pre-monsoon seasons (April—May). The TCs generated in the BoB generally move in a north-westerly direction during the post-monsoon season and northerly or north-easterly direction during the pre-monsoon season. The intensity of TCs gets modulated by mesoscale eddies. Hence, we have analysed the daily SLA data from AVISO to detect eddies and their interaction with Phailin and Fani. Figure 2a and b shows the five-day average SLA before (04—08 October 2013) and during (10—14 October 2013) the passage of Phailin.

A pre-existing cyclonic eddy evident in a closed-contour negative SLA can be seen in the western BoB near 86.5°E/17°N (Figure 2a). Phailin attained its peak intensity of category-5 TC near the BD10 mooring. It encountered a cyclonic eddy and subsequently weakened to a category-3 TC. However, in the case of Fani, a pre-existing anticyclonic eddy with a closed-contour positive SLA is present in the region of 82—87°E/15—17°N. Fani was a category-3 TC before encountering the anticyclonic eddy and intensified to a category-4 TC when it passed over the anticyclonic eddy. Mesoscale oceanic eddies can alter the surface SST signatures (Gaube et al., 2019). Also, SST plays a crucial role in determining TC intensity (Fisher, 1958). Hence, the role of the cyclonic and anticyclonic eddies on SST during the two TCs was investigated further.

3.3.2. SST

The energy required for the TCs comes from surface enthalpy fluxes (Emanuel, 1986), which depend on SST. Several studies (for example, Demaria and Kaplan, 1994) have documented the relationship between SST and the intensity of TC. Furthermore, SST uncertainty has been shown to play a significant role in errors in estimating and predicting TC intensity. The five-day averaged SSTfnd from GHRSST for Phailin and Fani is shown in Figure 3a—b and d—e, re-

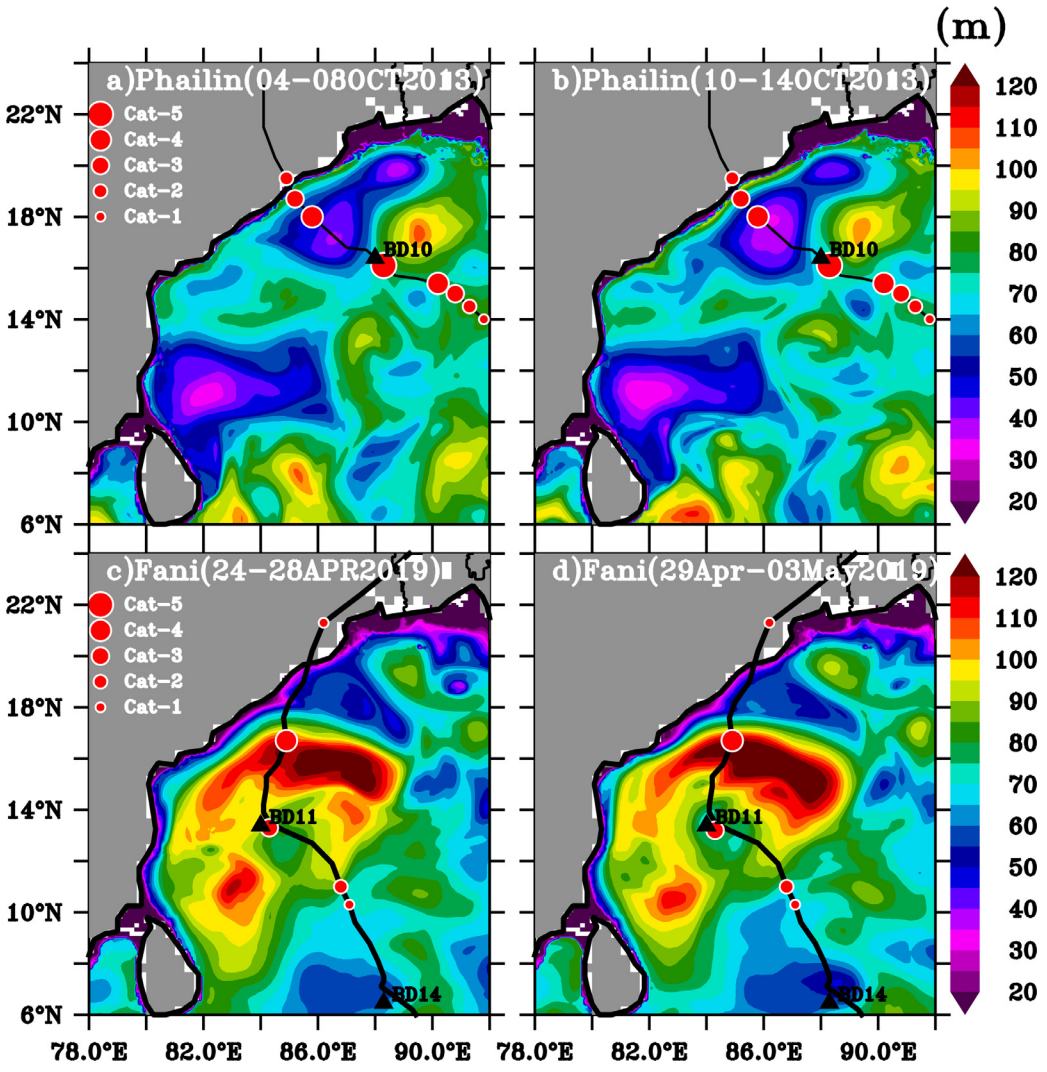

Figure 4 Five-day average D26 isotherm estimated from CMEMS data (a) during 04—08 October 2013, before the passage of Phailin, (b) during 10—14 October 2013, during the passage of Phailin, (c) during 24—28 April 2019, before the passage of Fani, and (d) during 29 April—03 May 2019, during the passage of Fani. The black triangular-shaped markers represent the moorings deployed by NIOT. The red circle-shaped markers indicate the intensity of the cyclone on the Saffir-Simpson scale.

spectively. The SST in the BoB prior to Phailin was greater than 29°C, which was consistent with moored buoy observations (Figures 3a and 1e). During Phailin, the SST cooling in the BoB was very small, 0.5°C (Figures 3b—c). Studies (Chaudhuri et al., 2019; Navaneeth et al., 2019) reported that the less cold wake during Phailin is due to salinity stratification. Sengupta et al. (2008) also reported that the SST cooling induced by the post-monsoon cyclones in the open north BoB is minimal. However, there was a significant cooling of 2.5°C in the areas where a cyclonic eddy was present (Figure 3c). Phailin weakened to a category-4 TC after passing through the cold wake. The entire BoB had a very warm SST (>30.5°C) prior to Fani (Figure 3d). The SST cooling was more pronounced in the regions south of 15°N (Figures 3e—f) during Fani. However, SST cooling was minimal in areas above 15°N (0.75°C). Also, note that Fani intensified into a category-4 TC in this region. To summarise, the passage of Phailin over the cyclonic eddy caused a significant SST cooling. The intensity of Phailin was found to be reduced from category-5 to category-3 during its passage over a cyclonic eddy. Contrastingly, Fani's passage over an anticyclonic eddy caused a weak cold wake. Also, Fani strengthened to category-4 from category-3 over the anticyclonic eddy. Gaube et al. (2019) documented that the cyclonic (anticyclonic) eddies result in shoaling (deepening) of mixed layers by eddy upwelling (downwelling). These subsurface changes induced by eddies can vary the TCHP and thereby affect the intensity of TC. Therefore, the subsurface ocean conditions during Phailin and Fani were investigated further to determine the causes of the intensity modulation of Phailin and Fani over eddies.

3.4. Subsurface ocean conditions

The energy required for a TC's intensification is provided by the ocean from the surface up to a depth in the range of 100—200 m (Lloyd & Veechi, 2011; Price, 1981; Shay et al.,

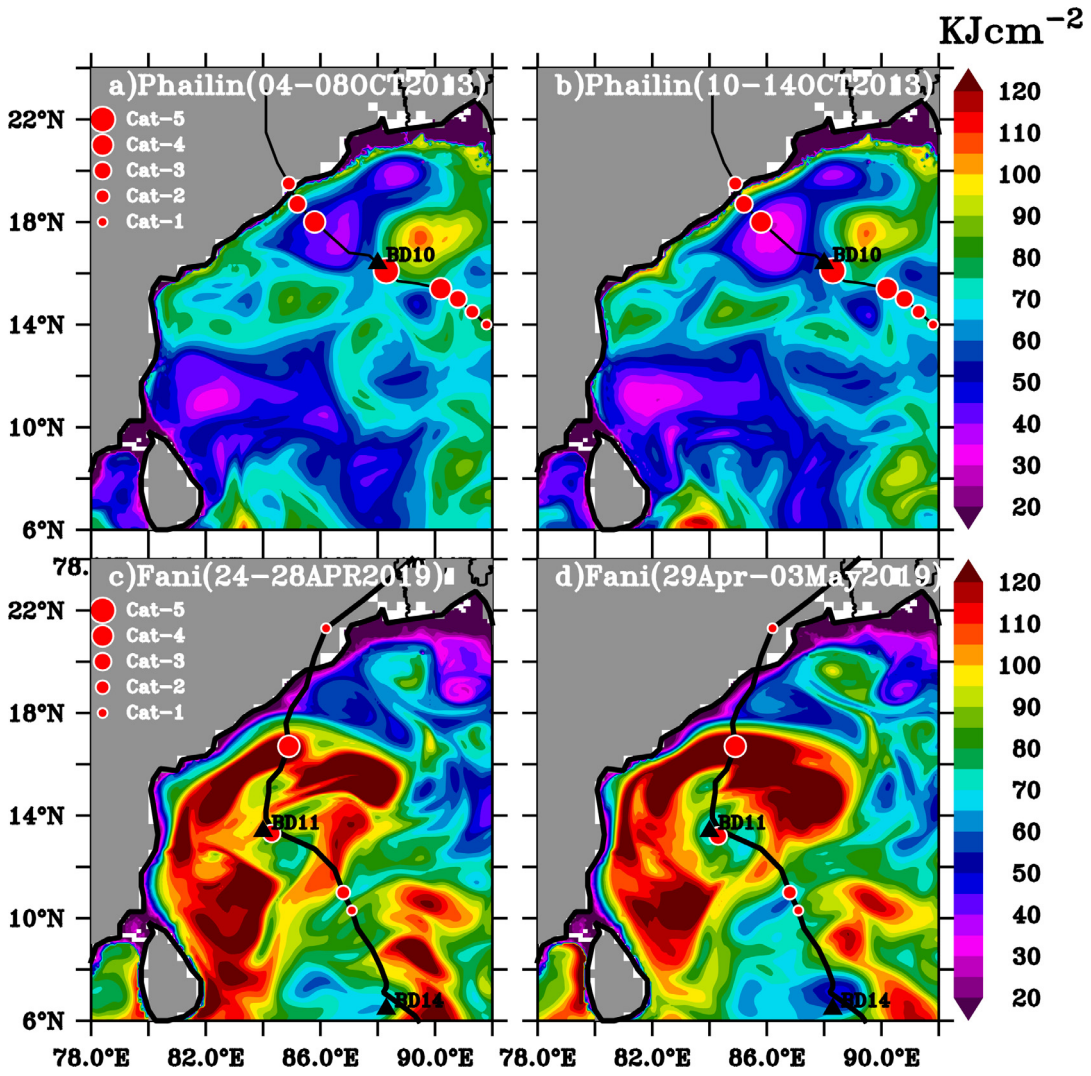

Figure 5 Five-day average TCHP estimated from CMEMS data (a) during 04—08 October 2013, before the passage of Phailin, (b) during 10—14 October 2013, during the passage of Phailin, (c) during 24—28 April 2019, before the passage of Fani, and (d) during 29 April—03 May 2019, during the passage of Fani. The black triangular-shaped markers represent the mooring deployed by NIOT. The red circle-shaped markers indicate the intensity of the cyclone on the Saffir-Simpson scale.

2000). The TCHP quantifies the thermal energy available below the ocean surface for the intensification of TC. TCs do not form in oceanic regions with SSTs less than 26°C. Hence, TCHP is estimated as the vertical integration of ocean temperatures above 26°C. Intensification of TC occurs in the regions of high TCHP (Wang and Wu, 2018). NOAA's Hurricane Centre has been using altimeter-derived TCHP data for operational forecasts since 2004 (Mainelli et al., 2008) and has reported that the forecasts are more accurate when using TCHP than SST alone. The D26 and TCHP values for Phailin and Fani, estimated from CMEMS, are shown in Figures 4 and 5, respectively.

The D26 isotherm can be considered as mid-thermocline depth, and the deepening (shoaling) of the D26 isotherm indicates downwelling (upwelling). The D26 isotherm was shallow (<40 m) in the cyclonic eddy region before Phailin (Figure 4a). When Phailin passed over the region of the cyclonic eddy, the cooler thermocline water is entrained into the mixed layer, lowering the SST (Figure 3c) compared to others. The shallow D26 also resulted in low TCHP values (<40 kJ cm^{-2}) before Phailin in the cyclonic eddy regions (Figures 4a and 5a). In situ temperature profiles from BD10 mooring also revealed a shallow D26 (~60 m) before the passage of Phailin cyclone (Figure 6a). The shallow D26 isotherm resulted in low TCHP values and significant SST cooling during the passage of Phailin over the cyclonic eddy. The cool SST and low TCHP over the regions of the cyclonic eddy supported the dampening of Phailin's intensity. However, during Fani, the region of the anticyclonic eddy was characterised by a deep D26 isotherm (>120 m) (Figure 4b) which indicates that the extension of the warmer temperature approaches 26°C up to 120 m depth, resulting in high TCHP values of ~140—180 kJ cm^{-2} (Figure 5b). Prior to Fani's passage, a deep D26 isotherm (90 m) was observed in the BD11 mooring (Figure 6b). The deep D26 isotherm resulted in high TCHP values and less cold wake over the anticyclonic eddy. The weak SST cooling and high TCHP provided a conducive environment for the intensification of Fani. SST

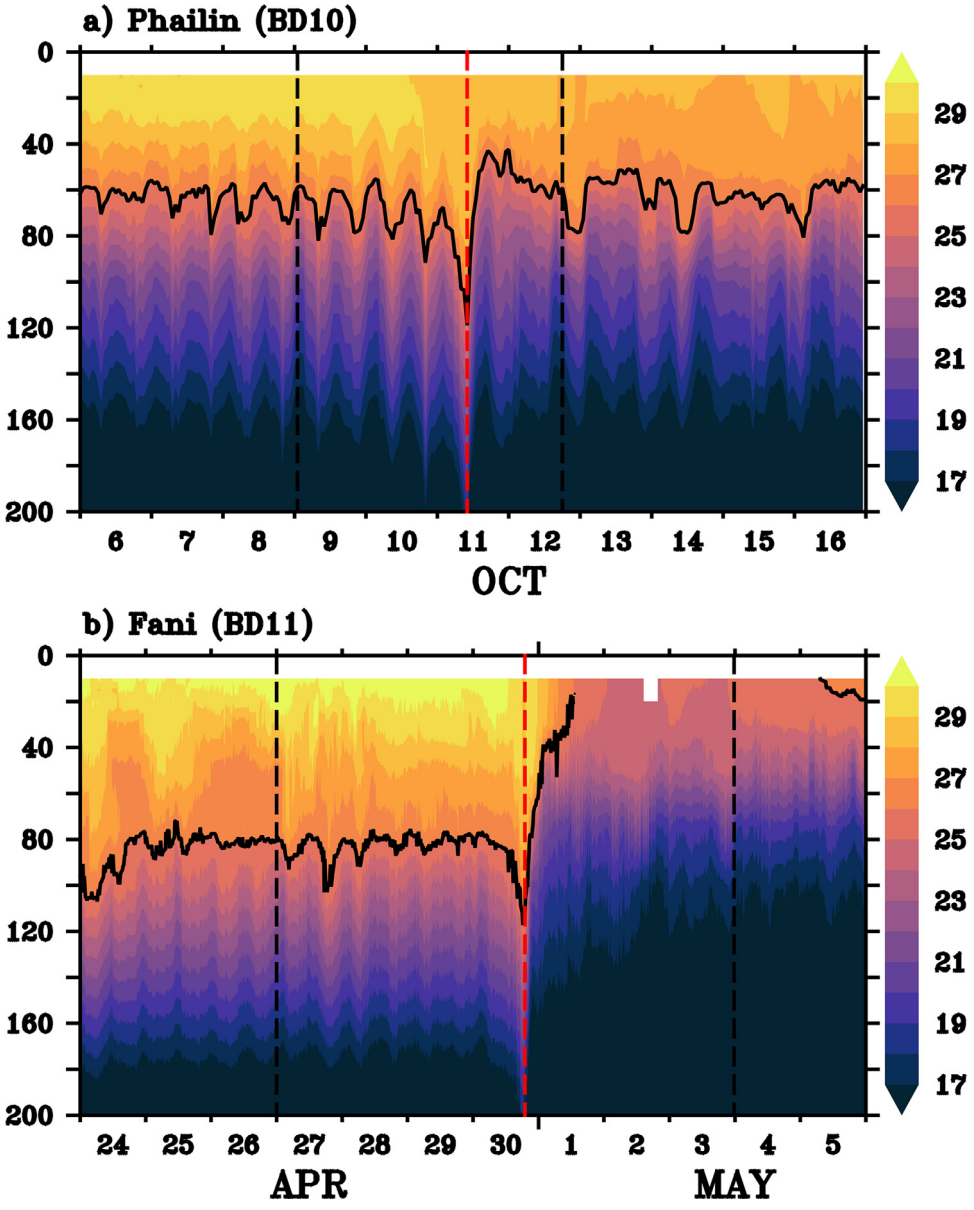

Figure 6 Temporal evolution of the vertical profile of temperature based on hourly moored buoy observations at a) BD10 during Phailin (2013) and b) BD11 during Fani (2019). The black line indicates the depth of the D26 isotherm in metres. The black dashed vertical lines represent the cyclone period and the red dashed lines indicate the time period where the cyclones were closest to the mooring locations.

patterns modulated by the oceanic eddies due to subsurface temperature variations can change the enthalpy fluxes at the air-sea interface. As the enthalpy fluxes control TC intensity (Emanuel, 1986; Emanuel et al., 2004; Riehl, 1954), the influence of the oceanic eddies on the enthalpy fluxes was further investigated.

3.5. LHF during Phailin and Fani

SST modulates the enthalpy fluxes (LHF + SHF) at the air-sea interface. The moisture and thermal disequilibrium at the air-sea interface are controlled by SST response. Studies by Cione and Uhlhorn (2003) revealed that SST cooling of approximately 1°C within the inner core of a TC could effectively change the maximum total enthalpy flux by 40% or more. Studies Ma et al. (2015) and Ma (2018) reported that the LHF rather than SHF has a significant role in fuelling storm intensification. The oceanic eddies modulated SST patterns during Phailin and Fani, which in turn could lead to variations in enthalpy fluxes. Hence, LHF and SHF variation during the two TCs was analysed. In order to study the eddy-TC interaction, ERA5 LHF and SHF data were temporally filtered using a 3—10 day Lanczos band-pass filter. Furthermore, a 2-D Gaussian high-pass filter with a cut-off wavelength of 600 km. The filtered LHF (LHF_{filt}) and SHF (SHF_{filt}) on October 12, 2013 and May 02, 2019 during Phailin and Fani were shown in Figures 7a—d. These two days were selected since the cyclones were located over eddies. The LHF_{filt} and SHF_{filt} showed positive values of ~20—30 W m^{-2} and ~3 W m^{-2} in the vicinity of the cyclone track located

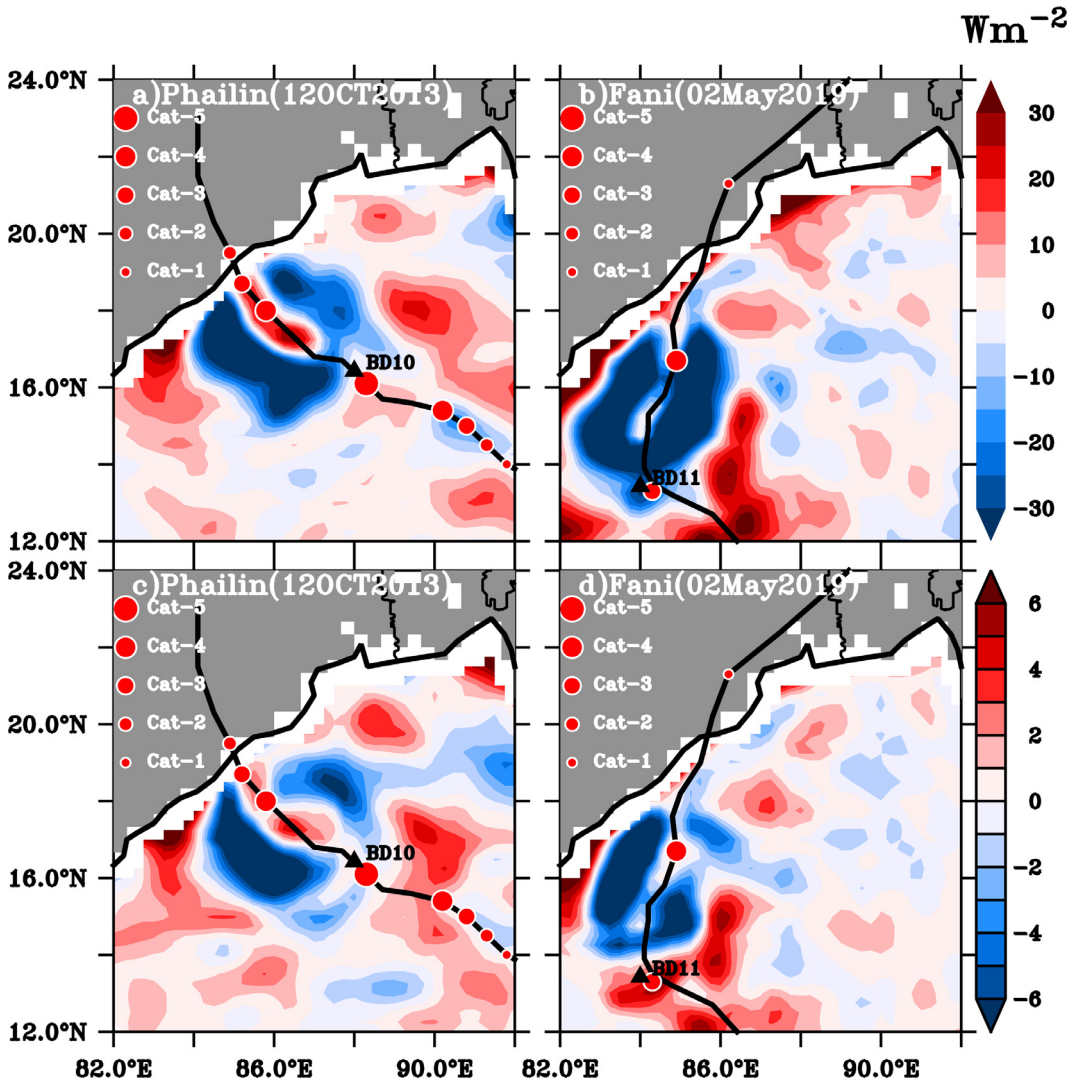

Figure 7 Filtered-LHF (LHF_{filt}) on (a) October 12th, 2013 (Phailin); (b) May 02, 2019 (Fani). Filtered-SHF (SHF_{filt}) on (c) October 12, 2013 (Phailin) and (d) May 2, 2019 (Fani).

within the cyclonic eddy on October 12th, 2013 (Figures 7a—c). The cold wake (Figure 3c) created due to the cyclonic eddy curtailed enthalpy fluxes and resulted in the weakening of Phailin. However, during Fani, LHF_{filt} showed negative values (~30 W m^{-2}) in the vicinity of the cyclone track situated within the anticyclonic eddy (Figure 7b). The meagre SST cooling (Figure 3f) due to the presence of anticyclonic eddy enhanced the LHF, which supported the intensification of Fani.

3.6. Atmospheric parameters (VWS, MTRH and Divergence at 200 hPa)

TC intensities are greatly affected by VWS (DeMaria and Kaplan 1999; Fitzpatrick 1997; Hanley et al. 2001). The low VWS between 950 and 200 hPa levels reduces the 'ventilation effect' of latent heat released in the cumulonimbus clouds in the core region of the TC. For intensification, VWS values less than ~10 m s^{-1} is conducive, with values between ~2 and 4 m s^{-1} favouring rapid intensification (Paterson et al., 2005). Hence, the role of VWS in modulating the intensity of Phailin and Fani is being investigated.

The Central Pressure (CP) and Maximum Sustained Winds (MSW) of Phailin and Fani, obtained from JTWC six-hourly track data, are shown in the Figure 8a and b respectively.

Phailin was a category-5 TC with a CP and MSW of ~922 hPa and 140 knots on October 11, 2013 before encountering the cyclonic eddy. The CP increased to 948 hPa and the MSW decreased to 100 knots on October 12, 2013, equivalent to a category-4 TC, after encountering the cold-core eddy. The VWS along Phailin's track is shown in Figure 8e. The VWS values were less than 9 m s^{-1}, after October 10, 2013, making them conducive for intensification. Also, the intensity of Phailin was at its maximum (category-5) during this time. Phailin encountered the cold-core eddy on October 11, 2013. Despite the fact that the VWS values were favourable for intensification (10 m s^{-1}), Phailin weakened to a category-4 TC. Figure 8c shows the SST cooling averaged over a 1° × 1° box centred on Phailin's track. Significant SST cooling (3°C) occurred in the vicinity of Phailin's

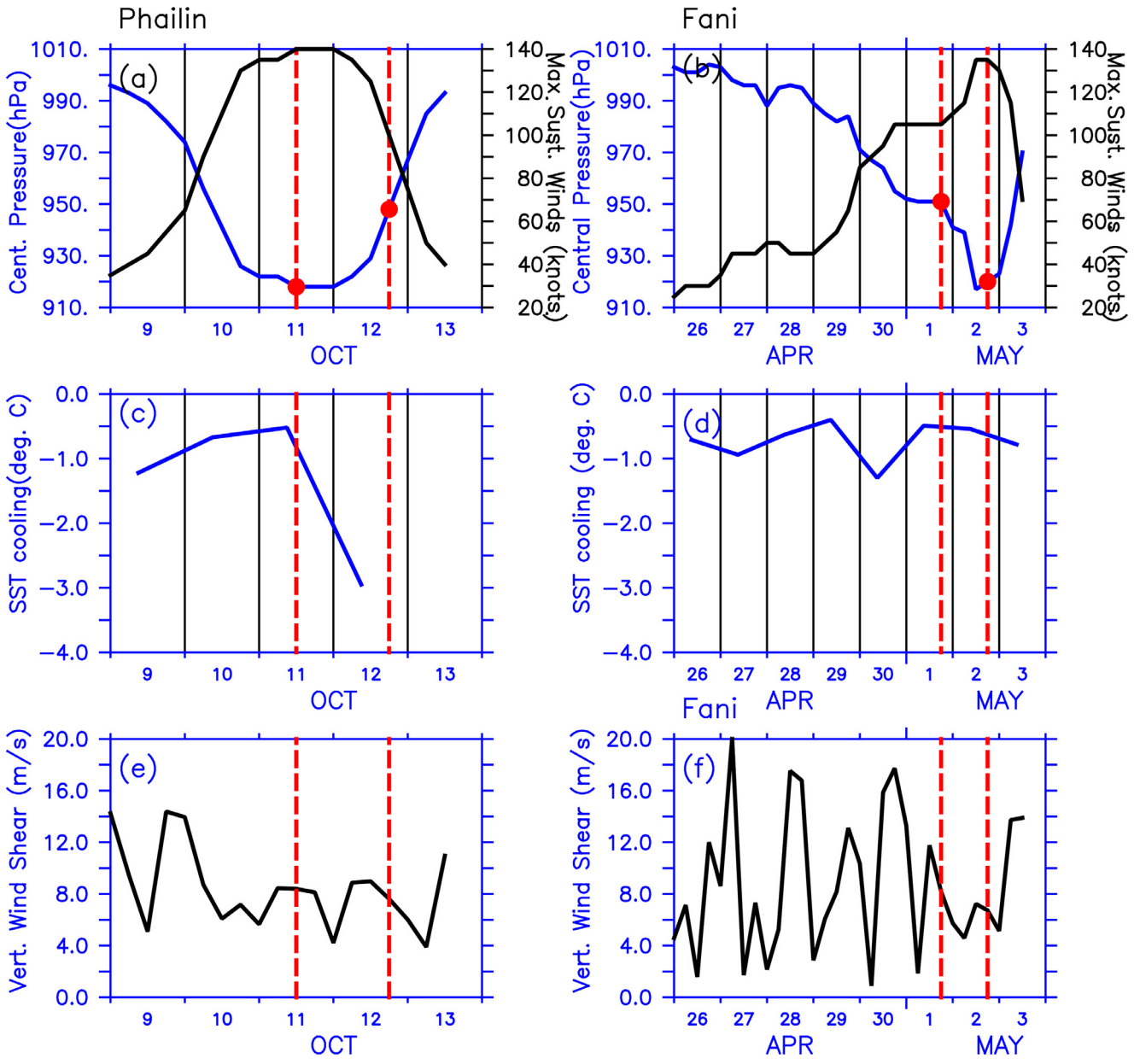

Figure 8 Central Pressure and Maximum Sustained Wind Speeds from JTWC track data (a) for Phailin and (b) for Fani. SST cooling averaged over a 1° × 1° box along the TC track (c) for Phailin and (d) for Fani. Vertical wind shear along the TC track (e) for Phailin (f) for Fani. The vertical red lines indicate the time of TC entering and leaving the eddy.

track in the areas of the cold-core eddy (Figures 3c and 8c). Strong cooling curtailed the supply of enthalpy fluxes (Figures 7a and c) dampening the intensity of Phailin.

Fani, on the other hand, was a Category 3 TC with a CP of ∼951 hPa and a MSW of ∼110 knots on May 01, 2019 (Figure 8b). The CP dropped to 917 hPa and the MSW increased to ∼135 knots after encountering the warm-core eddy. The VWS was ∼8 m s^{-1} when Fani encountered the warm-core eddy and remained less than ∼8 m s^{-1} favouring intensification (Figure 8f). Paterson et al. (2005) reported that values of VWS in this range will result in an intensification of ∼3 hPa. However, Fani experienced an intensification of ∼34 hPa. This suggests that VWS has only a minor effect on the intensification of Fani. The SST cooling averaged over a 1° × 1° box centred on the Fani's track is shown in Figure 8d. Weak SST cooling in the regions of warm-core eddy favoured the intensification of Fani (Figures 3f and 8d). The analysis of MTRH and divergence at 200 hPa during the pre-cyclonic days of Phailin and Fani has shown that these parameters have no significant contribution to modulating the intensity (Supplementary Figure S1).

4. Conclusions

The intensity modulation of TCs Phailin (2013) and Fani (2019) in the BoB is analysed in this study. Both the cyclones interacted with pre-existing mesoscale eddies before their landfall. The mesoscale eddies modulated the intensity of the two TCs. Phailin weakened to a category-3 TC

from a category-5 after encountering a cyclonic eddy. Contrastingly, Fani transected over an anticyclonic eddy and intensified. The surface and subsurface oceanic conditions in the BoB during the two TCs were analysed. The analysis revealed a pre-existing cyclonic eddy (SLA<25 cm) before the passage of Phailin. However, an anticyclonic eddy was present before the passage of Fani. Before Phailin, the SST in the BoB was 29.5°C. However, SST was much higher (>31°C) in the BoB before the onset of Fani. During Phailin, SST cooling in the BoB was minimal (1°C), with significant SST cooling (>2°C) restricted to cyclonic eddy regions. During Fani, significant SST cooling (>1°C) occurred south of 16°N. In contrast, the SST cooled very little (0.75°C) in the anticyclonic eddy regions.

The D26 isotherm and TCHP in the BoB during two TC periods were analysed to characterise the subsurface oceanic conditions. The D26 isotherm was observed to be shallower in the regions of cyclonic eddy compared to other regions in the BoB before the passage of Phailin. The TCHP values were also lower in the regions bounded by the cyclonic eddy due to shallow D26. Hence, significant SST cooling occurred in the regions confined by cyclonic eddy during the passage of Phailin, which favoured the weakening of Phailin. However, before Fani, the subsurface oceanic conditions in the regions of anticyclonic eddies were characterised by deep D26, which resulted in high TCHP. Hence, a weak SST cooling occurred in these regions during the passage of Fani. The weak SST cooling provided a conducive environment for the intensification of Fani over the anticyclonic eddy.

The enthalpy fluxes, especially LHF, play a significant role in controlling the TC intensity. Hence, LHF and SHF variations during the passage of two TCs over eddies were analysed. The LHF and SHF decreased by ∼20—30 W m^{-2} and ∼3 W m^{-2} respectively, in the region of the cyclonic eddy during Phailin on October 12, 2013. The analysis of VWS has shown that even though the shear was favourable for the intensification of Phailin, the strong SST cooling due to the cyclonic eddy curtailed the supply of enthalpy fluxes (especially LHF) and favoured the weakening of Phailin. Contrastingly, in the case of Fani, the weak SST cooling in the regions of anticyclonic eddy enhanced LHF supply from the ocean and favoured intensification. The estimates of VWS have shown that it played a minor role in Fani's intensification. The case study of the two TCs in the BoB has shown that the mesoscale oceanic eddies can modulate the intensity of TC. Hence, a thorough understanding of mesoscale eddies is vital for improving the accuracy of the TC intensity forecast.

Declaration of competing interest

The authors declare that they have no known competing financial interests or personal relationships that could have appeared to influence the work reported in this paper.

Acknowledgements

The authors thank the Ministry of Earth System Sciences, Govt. of India, for the support extended towards the moored buoy program. The authors are grateful to the Director, NIOT for the facilities and encouragement. The NIOT technical team is also acknowledged for maintaining the moored buoys.

Supplementary materials

Supplementary material associated with this article can be found, in the online version, at https://doi.org/10.1016/j.oceano.2022.02.005.

References

Babu, M.T., Sarma, Y.V.B., Murty, V.S.N., Vethamony, P., 2003. On the circulation in the Bay of Bengal during Northern spring intermonsoon (March—April 1987). Deep Sea Res. Pt. II 50, 855—865. https://doi.org/10.1016/S0967-0645(02)00609-4

Chaudhuri, D., Sengupta, D., D'Asaro, E., Venkatesan, R., Ravichandran, M., 2019. Response of the Salinity-Stratified Bay of Bengal to Cyclone Phailin. J. Phys. Oceanogr. 49, 1121—1140. https://doi.org/10.1175/JPO-D-18-0051.1

Chen, G., Wang, D., Hou, Y., 2012. The features and interannual variability mechanism of mesoscale eddies in the Bay of Bengal. Cont. Shelf Res. 47, 178—185. https://doi.org/10.1016/j.csr.2012.07.011

Cheng, X., McCreary, J.P., Qiu, B., Qi, Y., Du, Y., Chen, X., 2018. Dynamics of Eddy Generation in the Central Bay of Bengal. J. Geophys. Res. - Ocean 123, 6861—6875. https://doi.org/10.1029/2018JC014100

Cheng, X., Xie, S.-P., McCreary, J.P., Qi, Y., Du, Y., 2013. Intraseasonal variability of sea surface height in the Bay of Bengal. J. Geophys. Res. - Ocean 118, 816—830. https://doi.org/10.1002/jgrc.20075

Cione, J.J., Uhlhorn, E.W., 2003. Sea surface temperature variability in hurricanes: Implications with respect to intensity change. Mon. Waether Rev. 131, 1783—1796.

Demaria, M., Kaplan, J., 1994. Sea Surface Temperature and the Maximum Intensity of Atlantic Tropical Cyclones. J. Clim. 7, 1324—1334. https://doi.org/10.1175/1520-0442(1994)007<1324:SSTATM>2.0.CO;2

DeMaria, M., Kaplan, J., 1999. An updated statistical hurricane intensity prediction scheme (SHIPS) for the Atlantic and eastern North Pacific basins. Weather Forecast 14 (3), 326—337.

Donlon, C., Robinson, I., Casey, K.S., Vazquez-Cuervo, J., Armstrong, E., Arino, O., Gentemann, C., May, D., LeBorgne, P., Piollé, J., Barton, I., Beggs, H., Poulter, D.J.S., Merchant, C.J., Bingham, A., Heinz, S., Harris, A., Wick, G., Emery, B., Minnett, P., Evans, R., Llewellyn-Jones, D., Mutlow, C., Reynolds, R.W., Kawamura, H., Rayner, N., 2007. The Global Ocean Data Assimilation Experiment High-resolution Sea Surface Temperature Pilot Project. Bull. Am. Meteorol. Soc. 88, 1197—1214. https://doi.org/10.1175/BAMS-88-8-1197

Emanuel, K.A., 1986. An Air-Sea Interaction Theory for Tropical Cyclones. Part I: Steady-State Maintenance. J. Atmos. Sci. 43, 585—605. https://doi.org/10.1175/1520-0469(1986)043<0585:AASITF>2.0.CO;2

Emanuel, K.A., DesAutels, C., Holloway, C., Korty, R., 2004. Environmental Control of Tropical Cyclone Intensity. J. Atmos. Sci. 61, 843—858. https://doi.org/10.1175/1520-0469(2004)061<0843:ECOTCI>2.0.CO;2

Emanuel, K.A., 2013. Downscaling CMIP5 climate models shows increased tropical cyclone activity over the 21st century. PNAS 110 (30), 12219—12224. https://doi.org/10.1073/pnas.1301293110

Fisher, E.L., 1958. Hurricanes and the Sea-Surface Temperature Field. J. Atmos. Sci. 15, 328—333. https://doi.org/10.1175/1520-0469(1958)015<0328:HATSST>2.0.CO;2

Fitzpatrick, P.J., 1997. Understanding and forecasting tropical cyclone intensity change with the Typhoon Intensity Prediction Scheme (TIPS). Weather Forecast 12 (4), 826—846.

Gaube, P., J. McGillicuddy Jr., D., Moulin, A.J., 2019. Mesoscale Eddies Modulate Mixed Layer Depth Globally. Geophys. Res. Lett. 46, 1505—1512. https://doi.org/10.1029/2018GL080006

Hacker, P., Firing, E., Hummon, J., Gordon, A.L., Kindle, J.C., 1998. Bay of Bengal currents during the Northeast Monsoon. Geophys. Res. Lett. 25, 2769—2772. https://doi.org/10.1029/98GL52115

Halliwell, G.R., Gopalakrishnan, S., Marks, F., Willey, D., 2015. Idealized Study of Ocean Impacts on Tropical Cyclone Intensity Forecasts. Mon. Weather Rev. 143, 1142—1165. https://doi.org/10.1175/MWR-D-14-00022.1

Hanley, D., Molinari, J., Keyser, D., 2001. A composite study of the interactions between tropical cyclones and upper-tropospheric troughs. Mon. Weather Rev. 129 (10), 2570—2584.

Hersbach, H., Dee, D., 2016. ERA5 reanalysis is in production. ECMWF Newsl. 147, 5—6.

Jaimes, B., Shay, L.K., 2009. Mixed layer cooling in mesoscale oceanic eddies during Hurricanes Katrina and Rita. Mon. Weather Rev. 137, 4188—4207.

Kurien, P., Ikeda, M., Valsala, V.K., 2010. Mesoscale variability along the east coast of India in spring as revealed from satellite data and OGCM simulations. J. Oceanogr. 66, 273—289. https://doi.org/10.1007/s10872-010-0024-x

Li, Z., Yu, W., Li, T., Murty, V.S.N., Tangang, F., 2013. Bimodal character of cyclone climatology in the Bay of Bengal modulated by monsoon seasonal cycle. J. Climate 26 (3), 1033—1046.

Liang, J., Wu, L., Gu, G., 2018. Rapid Weakening of Tropical Cyclones in Monsoon Gyres over the Tropical Western North Pacific. J. Climate 31, 1015—1028. https://doi.org/10.1175/JCLI-D-16-0784.1

Liang, J., Wu, L., Gu, G., Liu, Q., 2016. Rapid weakening of Typhoon Chan-Hom (2015) in a monsoon gyre. J. Geophys. Res. Atmos. 121, 9508—9520. https://doi.org/10.1002/2016JD025214

Lin, I.-I., Chen, C.-H., Pun, I.-F., Liu, W.T., Wu, C.-C., 2009. Warm ocean anomaly, air sea fluxes, and the rapid intensification of tropical cyclone Nargis (2008). Geophys. Res. Lett. 36. https://doi.org/10.1029/2008GL035815

Lin, I.-I., Wu, C.-C., Emanuel, K.A., Lee, I.-H., Wu, C.-R., Pum, I.-F., 2005. The interaction of Supertyphoon Maemi with a warm ocean eddy. Mon. Waether Rev. 133, 2635—2649. https://doi.org/10.1175/MWR3005.1

Liu, Y., LÜ, H., Zhang, H., Cui, Y., Xing, X., 2021. Effects of ocean eddies on the tropical storm Roanu intensity in the Bay of Bengal. Plos one 16 (3), e0247521.

Lloyd, I.D., Vecchi, G.A., 2011. Observational Evidence for Oceanic Controls on Hurricane Intensity. J. Climate 24, 1138—1153. https://doi.org/10.1175/2010JCLI3763.1

Ma, Z., Fei, J., Huang, X., Cheng, X., 2015. Contributions of surface sensible heat fluxes to tropical cyclone. Part I: Evolution of tropical cyclone intensity and structure. J. Atmos. Sci. 72, 120—140. https://doi.org/10.1175/JAS-D-14-0199.1

Ma, Z., 2018. Examining the contribution of surface sensible heat flux induced sensible heating to tropical cyclone intensification from the balance dynamics theory. Dyn. Atmos. Oceans 84, 33—45. https://doi.org/10.1016/j.dynatmoce.2018.09.001

Ma, Z., Fei, J., Huang, X., Cheng, X., Liu, L., 2020. A Study of the Interaction between Typhoon Francisco (2013) and a Cold-Core Eddy. Part II: Boundary Layer Structures. J. Atmos. Sci. 77, 2865—2883. https://doi.org/10.1175/JAS-D-19-0339.1

Mainelli, M., DeMaria, M., Shay, L.K., Goni, G., 2008. Application of Oceanic Heat Content Estimation to Operational Forecasting of Recent Atlantic Category 5 Hurricanes. Weather Forecast 23, 3—16. https://doi.org/10.1175/2007WAF2006111.1

McTaggart-Cowan, R., Bosart, L.F., Davis, C.A., Atallah, E.H., Gyakum, J.R., Emanuel, K.A., 2006. Analysis of Hurricane Catarina (2004). Mon. Weather Rev. 134, 3029—3053.

Mei, W., Pasquero, C., 2013. Spatial and Temporal Characterization of Sea Surface Temperature Response to Tropical Cyclones. J. Climate 26, 3745—3765. https://doi.org/10.1175/JCLI-D-12-00125.1

Navaneeth, K.N., Martin, M.V, Joseph, K.J., Venkatesan, R., 2019. Contrasting the upper ocean response to two intense cyclones in the Bay of Bengal. Deep Sea Res. Pt. I 147, 65—78. https://doi.org/10.1016/j.dsr.2019.03.010

Neetu, S., Lengaigne, M., Vialard, J., Samson, G., Masson, S., Krishnamohan, K.S., Suresh, I., 2019. Premonsoon/postmonsoon Bay of Bengal tropical cyclones intensity: Role of air-sea coupling and large-scale background state. Geophys. Res. Lett. 46 (4), 2149—2157.

Paterson, L.A., Hanstrum, B.N., Davidson, N.E., Weber, H.C., 2005. Influence of environmental vertical wind shear on the intensity of hurricane-strength tropical cyclones in the Australian region. Mon. Weather Rev. 133 (12), 3644—3660.

Prasanna Kumar, S., Nuncio, M., Narvekar, J., Kumar, A., Sardesai, S., de Souza, S.N., Gauns, M., Ramaiah, N., Madhupratap, M., 2004. Are eddies nature's trigger to enhance biological productivity in the Bay of Bengal? Geophys. Res. Lett. 31, L07309. https://doi.org/10.1029/2003GL019274

Prasanna Kumar, S., Nuncio, M., Ramaiah, N., Sardesai, S., Narvekar, J., Fernandes, V., Paul, J.T., 2007. Eddy-mediated biological productivity in the Bay of Bengal during fall and spring intermonsoons. Deep Sea Res. Pt. I 54, 1619—1640. https://doi.org/10.1016/J.DSR.2007.06.002

Price, J.F., 1981. Upper ocean response to a hurricane. J. Phys. Oceanogr. 11 (2), 153—175.

Rappaport, E.N., Jiing, J.-G., Landsea, C.W., Murillo, S.T., Franklin, J.L., 2012. The Joint Hurricane Testbed: Its first decade of tropical cyclone research-to-operations activities reviewed. Bull. Amer. Meteor. Soc. 93, 371—380.

Riehl, H., 1954. Variations of energy exchange between sea and air in the trades. Weather 9, 335—340. https://doi.org/10.1002/j.1477-8696.1954.tb01706.x

Sadhuram, Y., Maneesha, K., Ramana Murty, T.V., 2012. Intensification of Aila (May 2009) due to a warm core eddy in the north Bay of Bengal. Nat. Hazards 63, 1515—1525. https://doi.org/10.1007/s11069-011-9837-1

Sengupta, D., Goddalehundi, B.R., Anitha, D.S., 2008. Cyclone-induced mixing does not cool SST in the post-monsoon north Bay of Bengal. Atmos. Sci. Lett. 9, 1—6. https://doi.org/10.1002/asl.162

Shay, L.K., Goni, G.J., Black, P.G., 2000. Effects of a Warm Oceanic Feature on Hurricane Opal. Mon. Weather Rev. 128, 1366—1383. https://doi.org/10.1175/1520-0493(2000)128<1366:EOAWOF>2.0.CO;2

Singh, V.K., Roxy, M.K., Deshpande, M., 2021. Role of warm ocean conditions and the MJO in the genesis and intensification of extremely severe cyclone Fani. Sci. Rep. 11, 3607. https://doi.org/10.1038/s41598-021-82680-9

Venkatesan, R., Shamji, V.R., Latha, G., Mathew, S., Rao, R.R., Muthiah, A., Atmanand, M.A., 2013. In situ ocean subsurface time-series measurements from OMNI buoy network in the Bay of Bengal. Current Sci. 104 (9), 1166—1177.

Vinayachandran, P.N., 2013. Impact of Physical Processes on Chlorophyll Distribution in the Bay of Bengal, Indian Ocean Biogeochemical Processes and Ecological Variability. Geophys. Monogr. Ser. https://doi.org/10.1029/2008GM000705

Wang, C., Wu, L., 2018. Future Changes of the Monsoon Trough: Sensitivity to Sea Surface Temperature Gradient and Implications for Tropical Cyclone Activity. Earth's Futur. 6, 919—936. https://doi.org/10.1029/2018EF000858